Microscale measurements reveal contrasting effects of photosynthesis and epiphytes on frictional drag on the surfaces of filamentous algae

AMY T. HANSEN*, MIKI HONDZO*, JIAN SHENG† AND MICHAEL J. SADOWSKY‡

St. Anthony Falls Laboratory, Department of Civil Engineering, University of Minnesota, Minneapolis, MN, U.S.A.
†*Department of Mechanical Engineering, Texas Tech University, Lubbock, TX, U.S.A.*
‡*Department of Soil, Water & Climate, Bio Technology Institute, University of Minnesota, St. Paul, MN, U.S.A.*

SUMMARY

1. Filamentous algae are widespread in freshwater ecosystems worldwide with a significant presence in streams, rivers and lakes with sufficient light and nutrients. Although typically not a preferred food source for grazers, dense filamentous mats provide surfaces for epiphytic microorganisms that are more palatable, thus adding to stream productivity.
2. We tested the hypothesis that epiphytes change velocity gradients, and consequently shear stress and skin friction drag, near the surface of algal filaments. Using both digital holography and particle image velocimetry to measure micrometre-scale velocity fields, we found that the surface shear stress on filamentous algae was much greater when the algae were actively photosynthesising. The presence of attached diatoms significantly reduced surface shear stress, while those filaments were photosynthesising, compared with bare filaments.
3. A nutrient flux model, based on boundary layer thickness and surface shear stress, predicts that nutrient flux to the surface of a photosynthesising filament under measured flow conditions will be 1.5 times greater than for a preserved (i.e. dead) filament. Modelled nutrient flux to filaments with epiphytic assemblages dominated by diatoms is 75% of the flux to bare filaments under similar flow conditions.
4. The proposed positive feedback between photosynthesis, surface shear stress and nutrient flux could be an important biophysical mechanism that overcomes diffusion limited nutrient supply within dense algal mats, enhancing algal survival through increased nutrient flux to actively photosynthesising filaments and decreased sloughing risk for filaments with lower rates of photosynthesis (due to epiphyte coverage or other light-limiting factors).

Keywords: *Cladophora*, diatoms, epiphytes, photosynthesis, skin friction

Introduction

Dense assemblages of filamentous algae, growing as algal mats, are key elements of stream aquatic habitat and contribute to stream production. Highly productive algal mats can have large effects on biogeochemical cycling by altering stream water nutrient and carbon concentration (Finlay *et al.*, 2011). By providing structural complexity and colonisable surface area, algal mats greatly enhance the abundance of stream microorganisms and have been referred to as stream area multipliers (Suren, 1991; Power *et al.*, 2009). Algal mats provide refuge to stream biota from potentially hazardous water currents and from fish predators (Dodds, 1991; Hart, 1992). Although filamentous algae are not themselves generally palatable to grazers, epiphytic microorganisms, including diatoms, bacteria and microalgae, are an important food source for grazers and, thus, filamentous algae are important in stream food webs (Dodds & Gudder, 1992; Power *et al.*, 2009).

The primary production of algal mats can be limited by light, nutrients and, before they are well established, grazing (Dodds & Gudder, 1992). Flow conditions can modify all of these. In turbulent flow, the supply of

---

Correspondence: Amy T. Hansen, St. Anthony Falls Laboratory, Department of Civil Engineering, University of Minnesota, Minneapolis, MN, U.S.A. E-mail: hanse782@umn.edu

dissolved nutrients and dissolved inorganic carbon to the algal surface is typically sufficient to support high productivity; under low-velocity conditions, however, algal growth is commonly limited by phosphorus or dissolved inorganic carbon (reviewed in Zulkifly *et al.*, 2013). At high flows (i.e. stream discharge), light availability may be decreased by increased suspended sediment (Leopold & Maddock, 1953). Epiphyte colonisation of algal filaments further compromises the availability of light and nutrients to the host. A complex three-dimensional structure can develop around individual filaments, often consisting of many layers of epiphytes that can intercept both light and nutrients (Lowe, Rosen & Kingston, 1982; Marks & Power, 2001). Young filaments, not yet heavily colonised, are vulnerable to grazers, which may then control mat biomass (Hart, 1992). Conversely, grazers have also been shown to release filamentous algae from the constraints imposed by epiphytes, by consuming the latter, essentially grooming the filaments (Dodds, 1991; Dudley, 1992).

Water movement within an algal mat has a strong effect on primary production by controlling mass transfer of nutrients and carbon to the plants, influencing immigration/emigration of both epiphytes and grazers and, at high velocity, inducing sloughing of algal tissue. Studies which have measured flow conditions within algal mats report an exponential decay in mean velocity with depth (Dodds & Biggs, 2002) and that flow within algal mats is more analogous to flow through porous media than to that through submerged aquatic macrophytes (Escartin & Aubrey, 1995). Reported velocity attenuation rates within the mat ranged from 0.29 to 0.96 mm^{-1} for four algal mats with minimal spatial variation in attenuation rates (Dodds & Biggs, 2002): At low velocity or in stagnant water, nutrient uptake rates can be faster than nutrient replenishment, and the reduced nutrient supply near the algal surface can limit physiological processes (Enriquez & Rodriguez-Roman, 2006; Hurd, 2000; Hurd, Harrison & Druehl, 1996; Wheeler, 1980). Although discussed conceptually by Larned, Nikora & Biggs (2004), the effect of fluid motion on nutrient uptake at low velocity has not been studied at the microscale at which cellular physiological uptake processes occur. At high in-stream velocity, physical damage to filamentous algae may occur, resulting in tissue sloughing (Biggs, Nikora & Snelder, 2005; Power, 1992). High velocity or storm events can enhance diatom and grazer immigration into the mat, as well as removing both grazers and attached epiphytes (Hardwick *et al.*, 1992; Schanz, Polte & Asmus, 2002; Stevenson & Peterson, 1991); all of which could have implications for mat productivity.

Epiphytes alter flow characteristics and nutrient availability within algal mats. In macroscale laboratory experiments with tufts of filamentous algae, epiphytes were found to decrease the drag coefficient for the tuft, which was attributed to reduced pore spacing (Dodds, 1991). Epiphytes may also change flow characteristics by altering surface roughness and surface wettability (i.e. hydrophobicity, hydrophilicity) due to differences in surface material or coatings compared with the host filament surface material, for example the frustule of silicate diatoms or excreted mucilage (Biggs & Hickey, 1994; Losic, Mitchell & Voelcker, 2009). The effect of epiphytes on nutrient availability is not well understood and will be the product of both passive and active changes in the local environment near the host algae surface. Epiphytes may decrease nutrient availability to the host algae by increasing the diffusion boundary layer thickness and physically blocking filament nutrient uptake (Sand-Jensen, Revsbech & Jorgensen, 1985) or may enhance nutrient availability by increasing surface roughness of the host vegetation (Koch, 1994). Epiphytes may compete for nutrients and light, thus decreasing availability to the host (Roberts *et al.*, 2003; Sand-Jensen *et al.*, 1985; Sand-Jensen, 1977), or a mutualistic nutrient cycle might exist, in which nutrient leaching from plant tissue benefits epiphytes and nutrient release from epiphytic microbial turnover is easily accessed by the plant, thus overcoming the otherwise nutrient-depleted boundary layer (Burkholder & Wetzel, 1990; Moeller, Burkholder & Wetzel, 1988). Epiphytes consist of a broad range of living organisms, both heterotrophic and autotrophic, so it is probable that the net effect of an epiphytic assemblage on the host vegetation depends on the composition of individuals in the assemblage (Eminson & Moss, 1980; Marks & Power, 2001).

Light availability also has a strong effect on algal mat productivity and decreases exponentially with depth within the mat (Borchart, 1996). Self-shading in dense algal mats was reported to be responsible for midsummer sloughing by weakening the tensile strength of filaments near the attachment point (Higgins, Hecky & Guildford, 2006). Despite the potential for self-shading within a mat, net photosynthesis generally increases with surface area to volume ratio for submerged aquatic vegetation and algal filaments have extremely high surface area to volume (Stewart & Carpenter, 2003). Macroscale studies which looked at net mat or canopy photosynthesis have reported that the primary effect of epiphytes on submerged aquatic vegetation, including filamentous algae, is increased shading, detrimental when light availability is limiting growth; (Drake, Dobbs

& Zimmerman, 2003; Koehler, Hachol & Hilt, 2010). Direct measurements of light attenuation by epiphytes on seagrass show that light attenuation increases with increasing epiphyte density and that the attenuation rate, approaching 100%, is dependent on epiphyte type (Brush & Nixon, 2002).

Here, we tested the hypothesis that epiphytes change the velocity gradient, and consequently shear at the surface of algal filaments. Microscale particle image velocimetry measurements were conducted under laboratory conditions within a range of flow conditions observed in the field. *Cladophora* filaments colonised by bacterial epiphytes, diatom epiphytes and without epiphyte colonisation were investigated. Specific objectives were to i) measure the effect of epiphytes on velocity gradients in the proximity of algal filaments; ii) measure the effect of light (absence or presence) on velocity gradients in the proximity of algal filaments; and iii) evaluate the potential effect of changed velocity gradients on nutrient transport in the proximity of algal filaments.

Methods

Field velocity measurements

To determine an appropriate velocity range for laboratory experiments, field velocity measurements were conducted within a mat of *Cladophora glomerata* in the Eel River (Angelo Range Research Reserve, CA, U.S.A.), on 23 June 2009 under typical summer baseflow conditions. This region experiences a Mediterranean climate, with rainy winters and dry summers (Power *et al.*, 2009). Under these conditions, *Cladophora* filaments can grow to >6 m in stretches of the river with high incident light, typically at locations with drainage areas greater than 100 km^2 (Finlay *et al.*, 2011; Power *et al.*, 2009). At the time of our measurements, *Cladophora* had not reached these sizes and the *Cladophora* mat height, h_c, was 0.25 m and water depth was 0.45 m; thus, the mat extended through somewhat over half the water column. Mat architecture was a dense, unordered array of filaments (Fig. 1a). Filaments were heavily colonised by diatoms: 96% of all epiphytes were microscopically identified to be the diatom *Cocconeis pediculus*.

Vertical velocity profiles were measured at one location in the middle of a large, dense *Cladophora* mat using a side-facing acoustic Doppler velocimeter (ADV) (Vectrino model, Nortek AS, Oslo, Norway). Field measurements were used to determine a
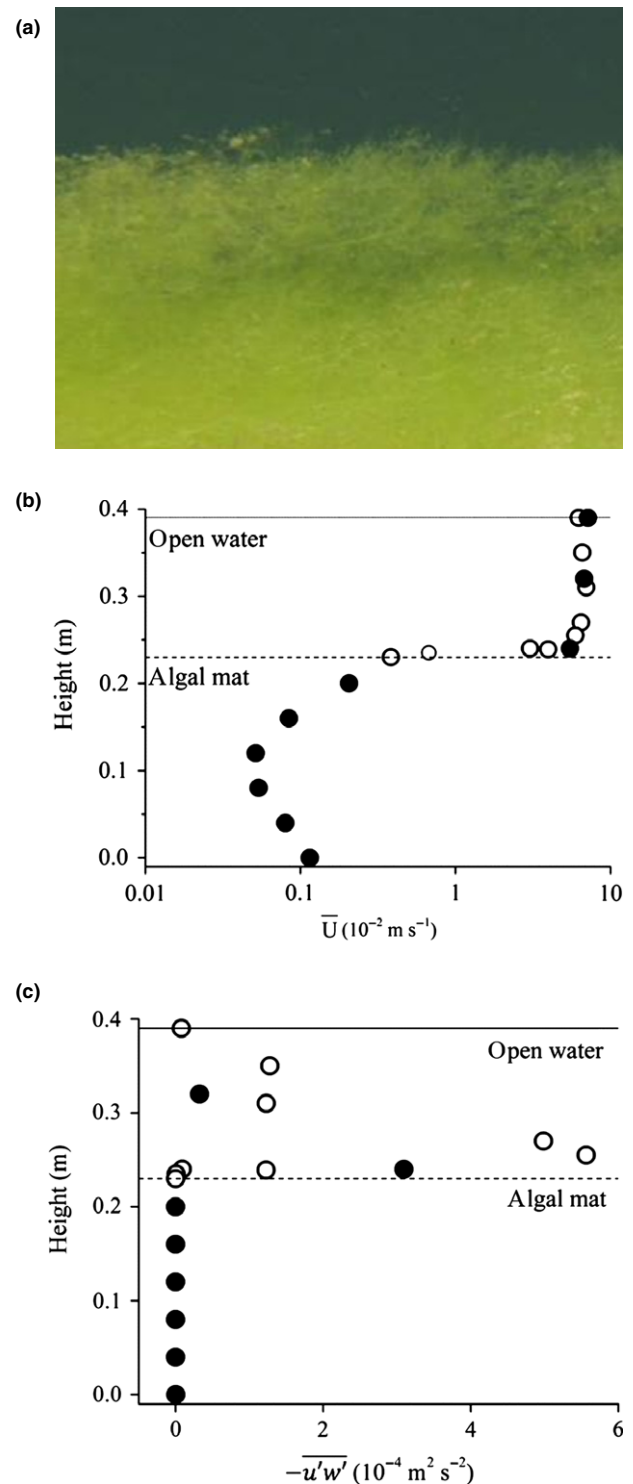
Fig. 1 (a) Underwater photograph illustrating structure of the *Cladophora* mat at the mat–open water interface; (b) Vertical time-averaged stream-wise velocity profiles through *Cladophora* mat. Open circles are from profile taken above the intact mat. An opening was cut into the mat then a second profile (solid circles) was taken through the entire water column; from the water surface, through the mat, to the sediment–water interface; (c) Profile of Reynolds stress, $-\overline{u'w'}$ (m^2 s^{-2}), measurements above and through the mat show that Reynolds stresses in the mat are negligible.

representative velocity range for designing laboratory experiments and not to characterise flow variability within mats. Flow variability within vegetative canopies (or mats) is highest in the vertical direction (Nepf, 2012; Raupach, Finnigan & Brunet, 1996), and therefore spatial variability in velocity was sampled with two vertical sequences. A velocity profile was first taken above the intact mat then, after cutting an opening, a second profile was taken through the mat to the sediment–water interface. This method, developed by Ikeda & Kanazawa (1996), has been used successfully by other researchers and is necessary for in-canopy ADV velocity measurements to avoid canopy interference within the measurement volume (Ghisalberti & Nepf, 2002, 2006; Plew, Cooper & Callaghan, 2008). At each vertical location, velocity was measured for 3 min at a sampling frequency of 200 Hz, resulting in 36,000 measurements per location. Measurement point spacing varied from 0.5 cm to 4 cm, with higher measurement point density near the top of the *Cladophora* mat to capture the anticipated velocity gradient. Time-averaged velocity, $\overline{U}$ (m s^{-1}) and the Reynolds stress, $-\overline{u'w'}$, (m^2 s^{-2}) were calculated for each measurement location and used to identify appropriate flow conditions for the laboratory experiments described below.

Laboratory sample preparation

Algal filaments used for microscale particle image velocimetry (μPIV) velocity measurements were selected to characterise three epiphyte treatments; epiphyte assemblages dominated either by diatoms, bacteria or no epiphytes (referred to as "bare"). Filaments with attached diatoms were *Cladophora* collected from the Eel River, CA, U.S.A. and from the Mississippi River, MN, U.S.A. Bare filaments and filaments with a bacterial biofilm were *Pithophora* cultured in a laboratory mesocosm where diatom growth was minimised by limited silicon supply in the growth medium, and bacterial growth was controlled with UV irradiation of the recirculating water (Badgley *et al.*, 2012). *Cladophora* and *Pithophora*, both members of the Cladophoreae family, are visually indistinguishable except under extremely unfavourable environmental conditions when special reproductive cells, that is, akinete cells, with distinct morphology develop (Spencer & Lembi, 1981). After collection, all filaments were stored in growth media at 4 °C for a maximum of 48 h. Cultured *Pithophora* were placed in a mixture of growth media and dead *Chlorophytum comosum* leaves until a bacterial biofilm developed for the filaments with a bacterial epiphyte treatment. Bacterial coverage for the

bacteria treatment and the absence of epiphytes for the bare treatment were both confirmed visually using a Nikon E400 light microscope with a 100× objective. For bare and diatom treatments, three filaments were used. For all other treatments, a single filament was used.

Velocity measurements were also made with bare algal filaments at three physiological states; live-light exposed, live-dark exposed, dead-light exposed. A single, cultured, bare *Pithophora* filament was used for the live-light and live-dark measurements. The dead-light-exposed measurements were made with a preserved, cultured, bare *Pithophora* filament, soaked in 70% ethanol for 16 h, rinsed, then stored at 4 °C. A control experiment was completed with a clean 304 stainless steel wire (127 μm diameter) in order to validate the analytical assumptions used to convert velocity gradient measurements to functional relationships between skin friction drag, C_D, and Reynolds number, Re.

Laboratory velocity measurements with particle image velocimetry

Fluid motion near the surface of individual algal filaments was characterised at a range of flow rates using μPIV (TSI Inc., Shoreview, MN, U.S.A.). A fluid consisting of 1 μm diameter neutrally buoyant fluorescent polystyrene latex spheres (Thermo Fisher Scientific Inc., Waltham, MA, U.S.A.) suspended in ultrapure water was pumped past individual filaments. Filaments were tethered in the centre of a high aspect ratio acrylic channel ($1 \times 0.06 \times 5$ cm). Image pairs were captured through an inverted microscope (Nikon Eclipse TE2000-S, Nikon, Tokyo, Japan) with a 10× DIC objective lens (Nikon Plan Fluor) using a double frame CCD camera (pixel size 6.5 μm, PIVCAM 14-10). The microscope objective was focussed at the filament surface at a depth corresponding to the centreline of the filament. Seed particles were illuminated by a double-pulsed Nd:YAG laser (532 nm emission wavelength). The displacement of each particle between images was determined by cross-correlation mapping of the two consecutive images over (96×96 pixel) interrogation windows covering a total mapped area of 300×450 μm. Using the computed displacement and known time interval between images, a velocity field was created for each image pair. These instantaneous velocity fields were time averaged across 200 measurements, using particle tracking and recognition techniques to account for individual particles (Fig. 2a).

For each filament, velocity fields were captured at flow rates ranging from 0.5 to 5.0 mL min^{-1}

(a)

(b)
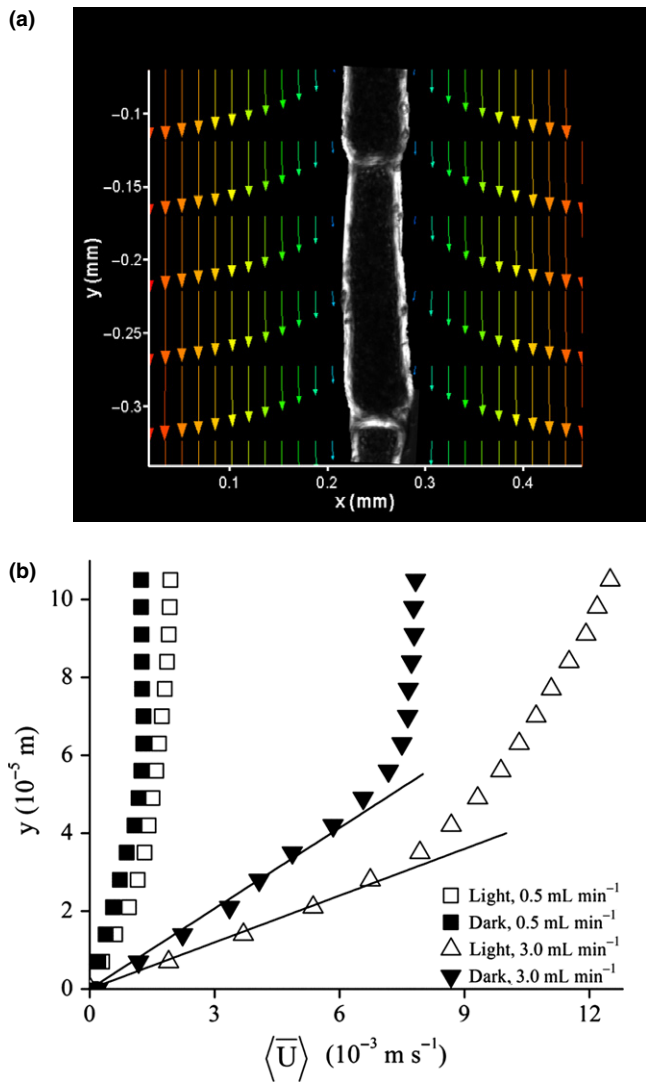
Fig. 2 (a) Example of a microscale particle image velocimetry (µPIV) time-averaged velocity field from which velocity gradients, shear stress and skin friction drag coefficient were calculated. A microscope image of an algal filament is superimposed on the velocity field, and only one-third of the velocity vectors are shown for clarity. (b) Temporally and spatially averaged velocity gradients from the digital holographic PIV system for the light versus dark experiment at two flow rates ($Q = 0.5$ mL min^{-1} and $Q = 3.0$ mL min^{-1}). The overbar represents time averaging, and the brackets represent spatial averaging. The y-axis is perpendicular to the flow direction and the algal filament. Velocity fields next to a single filament were measured for a range of flow rates under light-exposed conditions (open symbols) and dark-exposed conditions (solid symbols).

(± 0.05 mL min^{-1}). Experimental flow rates were controlled by a calibrated syringe pump (NE-500 model, New Era Pump Systems, Inc., NY, U.S.A.). The experimental range in flow rates was chosen such that the channel discharge velocity, U_D (m s^{-1}), where U_D is the flow rate divided by the cross-sectional area of the

channel, spanned the range in mean velocities measured *in situ* within the Eel River *Cladophora* mat. U_D ranged from 0.0014 to 0.014 m s^{-1}. Velocity fields were measured for nine algal filaments altogether and for a steel wire at various flow rates resulting in 57 measured velocity fields.

Laboratory measurements with digital holography

Due to the high energy and photosynthetically active wavelength of the µPIV laser, it was not possible to measure velocity fields with the µPIV without initiating photosynthesis. For this reason, the digital holographic system was used for experiments comparing velocity fields under light and dark conditions.

The light–dark experiment was conducted using a three-dimensional (3-D) digital holographic system, described in full detail in Sheng, Malkiel & Katz (2006), with a low-energy, long-wavelength laser (632.8 nm emission wavelength). Similar to the µPIV system described above, the digital holographic system measures velocity fields by comparing two images to track particle displacement over a known time interval. In this system, however, the laser light is split into two paths so that 3-D particle movement can be digitally reconstructed using depth information found in the interference fringes. To compare 3-D digital holographic measurements with the 2-D µPIV measurements, a 20-µm-deep slice was extracted from the 3-D volume data at the centreline of the filament and flattened. The channel and pump were identical to that used in the µPIV experiments. The flow was seeded with a sparse suspension of 2.9 µm latex microsphere particles (Thermo Fisher Scientific Inc.) in ultrapure water. Effective particle density for the analysis was increased by building surrogate images consisting of 30–90 actual images randomly selected and overlaid. Two hundred surrogate pairs were averaged to generate the time-averaged surface velocity fields.

The light–dark experiment was conducted using a single bare algal filament. After measuring velocity fields near the fresh, photosynthesising filament, the seed solution was pumped out of the channel and replaced with growth media. The filament was incubated in total darkness for the next 48 hr, after which the channel was again filled with seed solution and velocity fields were measured with the laser as the only light source. After the extended exposure to dark conditions, the experimental filament appeared brown; however, by exposing it to light until the chlorophyll appeared green (3 hr), it was verified to be alive and photosynthesising.

Calculation of shear stress and skin friction drag coefficient

Surface velocity gradients were determined from measured velocity fields and used to calculate shear stress and, in turn, the drag coefficient. A single, spatially and temporally averaged velocity gradient adjacent to the filament surface, $\langle \partial \bar{U}/\partial y \rangle$, where the overbar denotes time averaging and the brackets denote spatial averaging, was determined by averaging across all individual gradients within the camera's field of view (FOV) (μPIV: 20 gradients within FOV of 0.35 × 0.45 mm, holographic PIV: 113 gradients within FOV of 1.4 × 1.4 mm). Surface shear stress, τ_s (kg m^{-1} s^{-2}) where

$$\tau_s = \mu \left\langle \left. \frac{\partial \bar{U}}{\partial y} \right|_{y=0} \right\rangle \tag{1}$$

was determined from the velocity gradients near the filament surface where y is the vertical distance from the filament surface and μ (kg m^{-1} s^{-1}) is the fluid dynamic viscosity at 25 °C. Using τ_s, the fluid density ρ (kg m^{-3}), and the discharge velocity for the channel, the skin friction drag coefficient, C_D, was determined across a range in flow rates for each experiment where

$$C_D \equiv \frac{8\tau_s}{\rho U_D^2} \tag{2}$$

Flow conditions can be expressed non-dimensionally using the Reynolds number, Re, defined as:

$$\mathrm{Re} = \frac{U_D D_h}{v} \tag{3}$$

where v (m^2 s^{-1}) is the kinematic viscosity of the fluid, and D_h (m) is the hydraulic diameter of the channel. This definition of the hydraulic diameter neglects the contribution of the filament circumference which, for a 100 μm diameter filament, represents *c.* 1.4% of the total wetted diameter. Algal filament diameters, not including epiphytes, ranged from 80 to 150 μm. For each treatment, nonlinear least squares regression analysis was applied to determine the coefficient "*a*" in the power law equation,

$$C_D = a\mathrm{Re}^{-1} \tag{4}$$

The relationship between C_D and Re for steady, laminar flow through a closed rectangular channel can be determined analytically. For a height to width ratio of 0.06, as in our experimental set-up, C_DRe = 22.4 and for laminar, fully developed flow between two parallel plates, that is, plane Poiseuille flow, C_DRe = 24 (Kays, Crawford & Weigand, 2005; Shaughnessy, Katz & Schaffer, 2005).

This relationship has been confirmed to be singularly valid for a variety of materials and roughness conditions and is a single line for low Reynolds numbers on the well-known engineering graph, the Moody diagram (Moody, 1944). In other words, regardless of roughness or material properties, for laminar flow C_DRe is a function only of channel dimensions, physical fluid properties (i.e. viscosity) and velocity.

Nutrient flux model

A simple model of nutrient flux to the filament surface was developed to determine the effect of skin friction drag on nutrient uptake. At the algal surface, the nutrient flux, J_s (g m^{-2} s^{-1}), can be described as:

$$J_s = -D \left. \frac{\partial C}{\partial y} \right|_{y=0} \cong \frac{-D}{\delta_c} \Delta C \tag{5}$$

where D (m^2 s^{-1}) is the coefficient of diffusion of the nutrient in water, δ_c (m) is the concentration boundary layer thickness and ΔC (g m^{-3}) is the difference in nutrient concentration between the filament surface and the surrounding water within the algal mat. From scaling arguments presented in Steinberger & Hondzo (1999), the concentration boundary layer thickness can be estimated as:

$$\delta_c = c_1 \frac{v}{u_*} \mathrm{Sc}^{-1/3} \tag{6}$$

where u_* (m s^{-1}) is the shear velocity and Sc is the Schmidt number (Sc = v D^{-1}). The constant c_1 is empirically derived and typically found to be between 10 and 20 (Levich, 1962; Dade, 1993; Steinberger & Hondzo, 1999). Shear velocity, u_*, is defined as:

$$u_* \equiv \sqrt{\frac{\tau_s}{\rho}} \tag{7}$$

and can be expressed in terms of C_D using Eq. (2):

$$u_* = \frac{U_D}{2} \sqrt{0.5 C_D} \tag{8}$$

Substituting eqns 6 & 8 into eqn 5, J_s can be expressed in terms of C_D:

$$J_s = c_2 U_D \mathrm{Sc}^{-2/3} \Delta C \sqrt{C_D} \tag{9}$$

where $c_2 = \frac{-1}{c_1 \sqrt{8}}$ and the negative sign indicates that flux is into the filament surface. Eqn 9 can be rewritten in terms of Re, as:

$$J_s = \left[c_2 \frac{D^{2/3} v^{1/3}}{L} \Delta C \right] \mathrm{Re} \sqrt{C_D} \tag{10}$$

Results

In situ flow conditions

Average velocity within a mat of the filamentous alga *Cladophora glomerata* (Fig. 1a) at Angelo Coast Range Research Reserve (ACRRR) decreased from 0.065 m s^{-1} in the open water above the mat to 0.0005 m s^{-1} within it (Fig. 1b). Time-averaged, stream-wide velocity, $\overline{U}$ (m s^{-1}), within the *Cladophora* mat ranged from 0.0005 to 0.01 m s^{-1} (Fig. 1b); a decrease in over two orders of magnitude from the free-stream velocity to the lowest velocity within the mat. Within the same mat, Reynolds stresses, $-\overline{u'w'}$ (m^2 s^{-2}), which can be used to quantify the intensity of the flow turbulence, were negligible indicating laminar flow (Fig. 1c).

Laboratory experiments

Spatially and temporally averaged velocity gradients were constructed from μPIV and holographic PIV measurements of the velocity field near the surface of individual filaments within a closed channel (Fig. 2). C_D was determined from the slope of the gradients near the algal surface (illustrated in Fig. 2). For every treatment, C_D was inversely proportional to Re, that is, $b = -1$, resulting in a straight line on a log–log scale (Figs 3b & 4). The coefficient "a" is the product C_DRe and will be used to discuss experimental results and statistics (Table 1).

In our experiments, C_DRe calculated from velocity fields measured near a stainless steel wire resulted in the relationship C_DRe = 25 ($R^2 = 0.99$, $n = 5$), which agrees well with the analytically derived Poiseuille flow solution (C_DRe = 24). This close agreement indicated that error incurred from the experimental set-up was minimal. Results for the preserved algal filament (C_DRe = 27, $R^2 = 0.98$, $n = 4$) were also quite close to the analytical solution. However, for all live algal filaments, C_DRe was significantly greater than expected from the analytical solution for laminar flow through a closed rectangular channel (i.e. Poiseuille flow).

Epiphyte treatment

C_DRe values calculated from velocity measurements at the surface of live, light-exposed filaments with no epiphytes collapsed to C_DRe = 60 ($R^2 = 0.98$, $n = 16$: Fig. 3b) as did filaments with bacterial epiphytes ($R^2 = 0.99$, $n = 7$: Fig. 3b). This coefficient is over two times greater than expected for Poiseuille flow and than

Wire   Diatoms   Bacteria   Diatoms   Diatoms
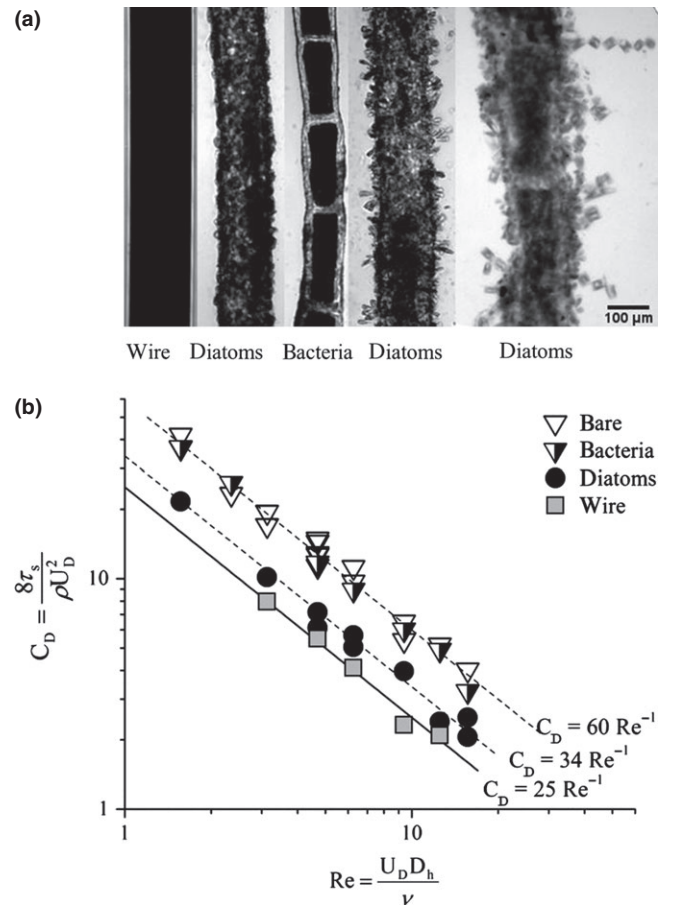
Fig. 3 (a) Microscope images of a representative sample of filaments used for the laboratory experiments; stainless steel wire (i), *Cocconeis spp.* diatom-dominated assemblage (ii), bacterial biofilm assemblage (iii), mixed diatom assemblage (iv), mixed diatom/bacteria assemblage (v). (b) Experimental results demonstrating the relationship between the skin friction drag coefficient, C_D, and the Reynolds number, Re.

calculated for the steel wire. No difference was seen between filaments without epiphytes and filaments with bacterial epiphytes. Calculated C_DRe from experimental velocity measurements near filaments with diatom epiphytes resulted in C_DRe = 34 ($R^2 = 0.99$, $n = 10$, Fig. 3b), 56% of what was determined for live, light-exposed filaments without diatom epiphytes and still much greater than predicted by laminar flow theory (Fig. 3b).

Physiological state

To determine whether observed differences in velocity fields and resulting C_DRe among treatments were due to photosynthesis, velocity field measurements were taken near the surface of a single live bare filament using digital holographic particle image velocimetry and a

Table 1 Summary of laboratory experimental results

	Method	a	b	n	R^2	J/J_{ref}
Epiphyte treatment						
Bare	μPIV	60.45	−1.00	16	0.98	1.59
Bacteria	μPIV	59.81	−1.03	7	0.99	1.58
Diatoms	μPIV	33.93	−1.02	10	0.99	1.19
Physiological state						
Live-light	holoPIV	61.74	−0.97	5	0.99	1.61
Live-dark	holoPIV	39.86	−0.97	4	0.99	1.29
Preserved light	μPIV	28.59	−1.06	4	0.97	1.09
Wire	μPIV	25.35	−1.01	5	0.99	1.03
Analytical solution (Poiseuille flow)						
		24.00	−1.00	–	–	1.00

Nonlinear regression was used to fit C_D versus Re data to an equation of the form $y = ax^b$, where a is a constant coefficient, b is a constant exponential coefficient, n is the number of measurements and R^2 is an adjusted R for nonlinear least squares regression. Nutrient flux calculations are referenced to the analytical solution for Poiseuille flow.
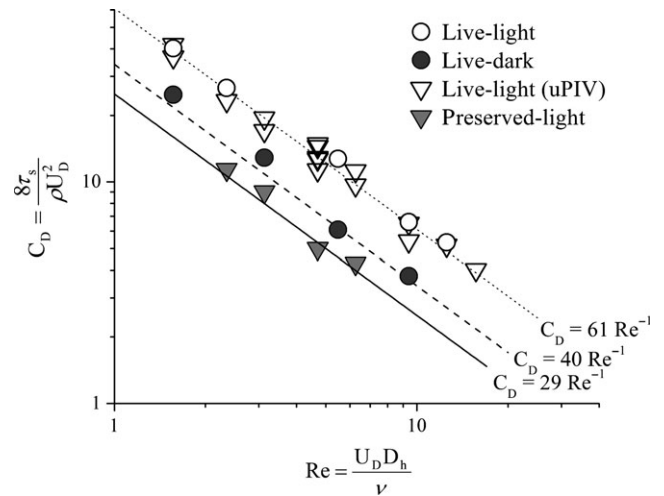μPIV, microscale particle image velocimetry.

low-energy high-wavelength laser after both light and dark incubations. Under light-exposed conditions, C_DRe = 62 (R^2 = 0.99, n = 5), very similar to results for bare live filaments measured with μPIV system (Fig. 4). After 48 h of dark incubation, C_DRe = 40 (R^2 = 0.99, n = 4, Fig. 4). This indicates that, under similar fluid flow conditions, skin friction drag was much less at the surface of the dark-incubated filament than it was for the same filament exposed to light. Under both light and dark conditions, skin friction drag was still higher than measured for the preserved filament (Fig. 4).
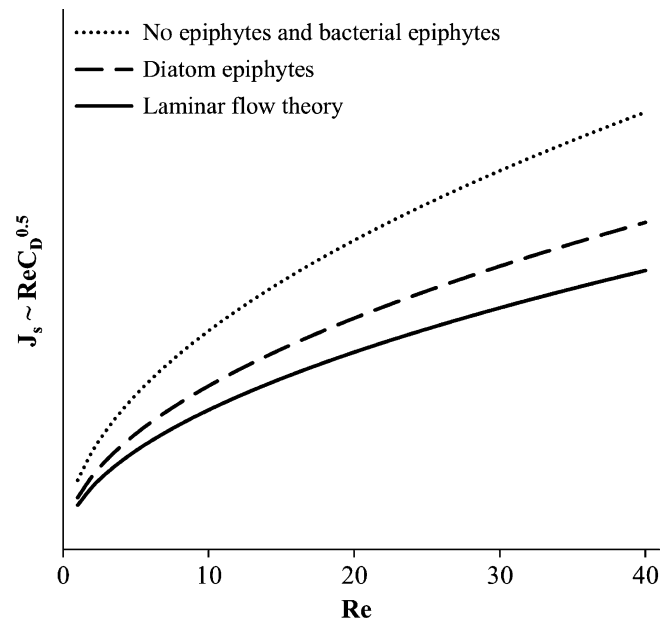
Nutrient flux

Nutrient flux to the algal surface was evaluated using eqn 10, and the experimentally derived relationships C_D versus Re shown in Figs 3 & 4 and summarised in Table 1. Assuming physical water properties and dissolved nutrient concentration are the same for all treatments (i.e. the variables in the square brackets in eqn 10) and that nutrient supply limits algal nutrient uptake, then nutrient uptake for each treatment can be evaluated relative to a reference treatment by examining the ratio.

Nutrient flux to a live, photosynthesising algal filament was calculated to be 1.5 times greater than flux to a non-photosynthesising filament for all Re, due to the boundary layer thinning under the higher surface shear stress during photosynthesis (Table 1, Fig. 5). Similarly, by comparing the ratio of nutrient flux to the surface of a filament with diatom epiphytes to the flux to a bare fil-

Fig. 4 Reynolds number versus skin friction drag coefficient from digital holographic particle image velocimetry (PIV) experiment comparing velocity fields measured after light incubation and dark incubation for the same filament. For comparison, regression lines are shown from the μPIV results in Fig. 3 including the analytical solution (solid line), filaments with diatom-dominated epiphyte assemblages (large dashes) and filaments with bare or bacterial-dominated epiphyte assemblages (small dashes).

Fig. 5 Modelled filament surface nutrient flux J_s, as a function of Reynolds number for the analytical, laminar flow theory solution (solid line), filaments with diatom-dominated epiphyte assemblages (large dashes) and filaments with bare or bacterial-dominated epiphyte assemblages (small dashes).

ament, diatom epiphytes are expected to decrease nutrient availability at the filament surface by 25% due only to changes in the velocity field (Fig. 5). Bacterial epi-

phytes were not observed to modify Re versus C_D in our experiments and are thus not expected to affect nutrient flux to the algal surface.

Discussion

Our original hypothesis, that epiphytes will change velocity gradients in the proximity of algal filaments, was partially supported by our results: diatom epiphytes did increase velocity gradients and thus shear stress, although bacterial epiphytes did not. Surprisingly, velocity gradients at the surface of algal filaments with no epiphytes were much higher than predicted by laminar flow theory (i.e. Poiseuille flow), and suggest that one of the assumptions of Poiseuille flow (i.e. no slip at the wall and constant fluid material properties) was invalid for live, photosynthesising algal filaments. Based on measured velocity gradients, nutrient flux to a photosynthesising algal surface would be 1.6 times greater than predicted by laminar flow theory (Table 1).

Average measured velocity within the *Cladophora* mat ranged from 0.0005 to 0.01 m s^{-1} (Fig. 1b), well within the laminar flow range (e.g. Kays *et al.*, 2005). This velocity range is similar to previously reported measurements in algal mats (Dodds & Biggs, 2002; Escartin & Aubrey, 1995) and much lower than velocities within four types of aquatic plant canopies, which were greater than 0.02 m s^{-1} for 88% of measurements (Sand-Jensen & Pedersen, 1999). At a velocity lower than 0.02 m s^{-1}, productivity is expected to be limited by mass transfer of nutrients and carbon (Dodds, 1991). However, filamentous algae are notoriously productive despite potential mass transfer limitation of nutrient supply within dense mats. The results presented here, which show that skin friction drag is 1.5 times greater for photosynthesing than preserved filaments, may help explain the paradoxically high productivity of filamentous algal mats under low-velocity conditions. Nutrient flux calculations suggest that higher skin drag, which decreases boundary layer thickness, allows nutrient to be replenished 1.5 times faster near the surface of a photosynthesising filament than would be expected from laminar flow theory. These results have profound implications for nutrient replenishment within an algal mat and suggest that filamentous algae have a previously unknown adaptation to their environment that enhances survival and fitness. By actively increasing skin friction drag, nutrient flux to the algal surface is greatest when the filament is photosynthesising. High surface shear stress during photosynthesis may also enhance removal of loosely attached epiphytes and detritus (Harvey *et al.*, 2011), which again

increases light availability. When not actively photosynthesising, as in filaments near the bottom of the mat in poor light conditions or where incident light is otherwise reduced, skin friction drag is less.

Epiphytic assemblages dominated by diatoms decreased skin friction drag compared with bare filaments, supporting our original hypothesis that epiphytes change velocity gradients close to the algal surface. Diatoms assemblages can cover large areas of the filament and alter light availability to the host, surface wettability and may physically block gas exchange by the filament (Biggs & Hickey, 1994; Drake *et al.*, 2003). Previous studies at the vegetative mat scale found that diatom assemblages decreased drag (Dodds, 1991) and decreased the rate of photosynthesis (Drake *et al.*, 2003; Koehler *et al.*, 2010; Sand-Jensen, 1977), although no studies have simultaneously examined both variables. Our results, obtained at the microscopic scale and consistent with both light and fluid macroscale results, show that diatoms decreased filament skin friction drag and that this was due to decreased photosynthesis. Nutrient flux to the surface of filaments covered by diatoms is expected to be 75% of that for bare filaments (Table 1). It is not possible to conclude from this study whether diatoms interrupt photosynthesis by blocking gas exchange or incident light. Reduced surface drag could decrease rates of diatom detachment (Dodds, 1991) but also decrease nutrient replenishment.

Velocity gradients were not significantly different between filaments without epiphytes and those with bacterial epiphytes, suggesting the latter did not have an effect on skin friction drag (Fig. 3b). Although direct measurement of velocity fields for filaments with only bacterial epiphytes was limited to one filament, further support for this conclusion is evident in the results from the diatom treatment. Diatom-dominated epiphytic assemblages varied in their bacterial composition; for example, Mississippi River filaments had a high abundance of bacteria while ACRRR filaments had less bacteria, but all filaments with diatom epiphytes behaved similarly (Fig. 3b). Further analysis is required to confirm the effect of bacterial epiphytes on skin friction drag across varying bacterial densities, types and with a larger number of filament samples.

This study, conducted with single filaments under laboratory conditions, indicated that velocity gradients, and thus surface shear stress and skin friction drag, are greater for photosynthesising filaments than filaments which are not photosynthesising, and that diatoms decrease skin friction drag. However, algal mats are composed of thousands of individual flexible filaments.

Meaningful interpretation of our results at a mat or stream-reach scale requires further investigation using a number of filaments under a range of flow conditions (Sand-Jensen, Binzer & Middelboe, 2007). Within an algal mat, filaments may not be oriented in the direction of the flow, and spacing between the filaments may be small enough for the boundary layers to overlap; both which could change the scale at which velocity gradients respond to photosynthesis. Additionally, this study assumed that the dissolved nutrients in the water column were the only nutrient source. There are likely to be important interactions between epiphytes and filaments, either competitive or mutualistic, that are not captured in our nutrient flux model but would have to be quantified to interpret our results in the context of stream-reach scale biogeochemical processes.

At present, we cannot confirm the unique mechanism through which photosynthesis increased surface shear stress and skin friction drag. Reported mechanisms that increase microscale surface shear stress under laminar flow conditions include surface roughness and hydrophobicity, and the presence of a surface gas layer (reviewed in Neto *et al.*, 2005). Surface roughness did not have a measurable effect on surface shear stresses or skin friction drag in this experiment, despite having been reported to change surface shear stresses at microscales (Harting, Kunert & Hyvaluoma, 2010) and to increase drag forces in macroscale turbulent flows, as classically shown in the Moody diagram (Moody, 1944). If roughness had been responsible for the observed increase in surface shear stress, then the smooth, bare algal filaments should have behaved more like the stainless steel wires than like the filaments with diatom assemblages, which are much rougher. Additionally, if roughness had been responsible for increased surface shear stress, the preserved filament and dark-exposed filaments would have behaved the same as the live, light-exposed filaments. Surface hydrophobicity was not measured but, again, if surface hydrophobicity had been responsible for increased surface shear stress, the preserved filament and dark-exposed filament would have behaved the same as the live, light-exposed filaments. Of these three reported mechanisms, we suggest that the raised surface shear stresses observed in our experiments for live algal filaments resulted from changes in local viscosity or bubble formation, due to high rates of oxygen production at the filament surface.

Photosynthetically increased drag may be due to the formation of small, stable bubbles within the supersaturated oxygen concentrations in the boundary layer near the filament. Both oxygen supersaturated water and oxygen-

rich bubbles are known to increase the effective viscosity of the near-surface fluid in low Reynolds number flows, resulting in a larger drag coefficient (Valukina & Kashinskii, 1979; Pal, 2007). Stable, oxygen-rich, microscale bubbles have been previously reported to form in photosynthetic microbial mats at dissolved oxygen concentrations of 200 μmol L^{-1} (Bosak *et al.*, 2010). For comparison, in the algal mat where field velocity measurements were taken, dissolved oxygen concentrations were ~300 μmol L^{-1} at midday, well above the threshold for bubble formation. Additionally, based on laboratory measurements, oxygen was released from the filamentous algae *Pithophora* into water at a rate of 5.6 mg O_2 h^{-1} (g DW)$^{-1}$ (Hansen & Hondzo, unpublished data). This is similar to field measured flux rates in *Cladophora* mats across five sites in eastern Lake Erie that averaged 6.9 mg O_2 h^{-1} (g DW)$^{-1}$ (Higgins, Hecky & Guildford, 2008) and in the middle of the range of photosynthetic rates summarised in a meta-analysis of submerged aquatic vegetation (Binzer, Sand-Jensen & Middelboe, 2006). At this flux rate, after 1 h, the oxygen concentration in the experimental channel would be sufficient for bubbles to form. Neither the μPIV system nor the digital holographic system had high enough magnification to visually verify bubbles during experimental measurements. In a separate set-up using an optical microscope and a 60$\times$ objective, bubble forma-
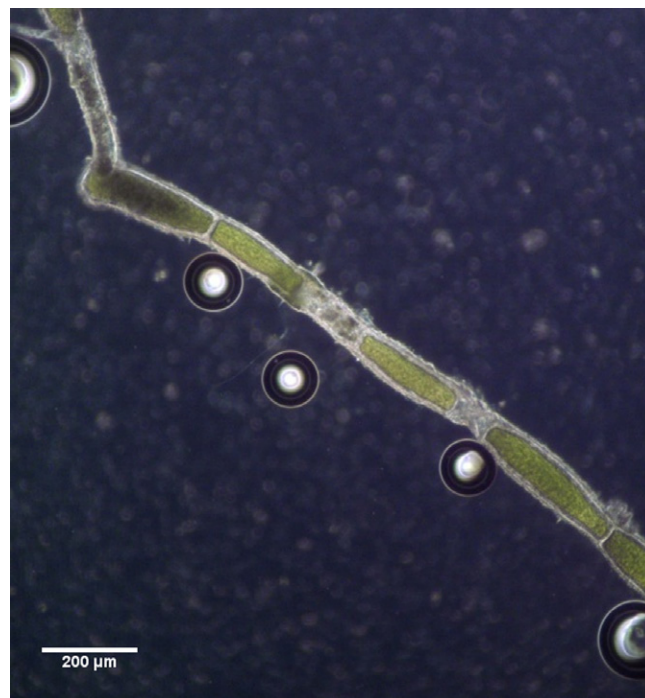

Fig. 6 Microscopic image of bubbles formed at surface of *Pithophora* filament after 3 h light exposure in solution of growth media and 1 μm seed particles.

tion was recorded after 3 h in sealed microscope slides with a single filament in a 10% seeding solution in growth medium (Fig. 6). In the same experiment, bubbles did not form in slides prepared with stainless steel wire or in slides with pure growth medium, possibly due to lack of nucleation sites. Suspended sediment could provide bubble nucleation sites in the field.

In conclusion, through microscale velocity measurements near the surface of algal filaments, shear stress and thus skin friction drag were shown to be 1.5 times greater for photosynthesising filaments than for preserved filaments. Modelled flux rates based on analytical expressions for Poiseuille flow greatly underestimated nutrient flux to the filament surface. The presence of diatoms decreased surface shear stress, skin friction drag and nutrient availability compared with bare, photosynthesising filaments. These results suggest that *Cladophora, Pithophora* and possibly other filamentous mat-forming algal species can overcome the physical and physiological constraints on nutrient supply imposed by low flow rates through dense filament assemblages. Understanding how mat-forming algal species persist in the natural environment could provide valuable insight into the ecology and biogeochemistry of streams dominated by such mats.

Acknowledgements

References

Badgley B.D., Ferguson J., Hou Z. & Sadowsky M.J. (2012) A model laboratory system to study the synergistic interaction and growth of environmental *Escherichia coli* with macrophytic green algae. *Journal of Great Lakes Research*, **38**, 390–395.

Biggs B.J.F. & Hickey C.W. (1994) Periphyton responses to a hydraulic gradient in a regulated river in New Zealand. *Freshwater Biology*, **32**, 49–59.

Biggs B.J.F., Nikora V.I. & Snelder T.H. (2005) Linking scales of flow variability to lotic ecosystem structure and function. *River Research and Applications*, **21**, 283–298.

Binzer T., Sand-Jensen K. & Middelboe A.L. (2006) Community photosynthesis of aquatic macrophytes. *Limnology and Oceanography*, **51**, 2722–2733.

Borchart M.A. (1996) Nutrients in algal ecology. In: *Algal Ecology* (Eds R.J. Stevenson, M.L. Bothwell & R.L. Lowe), p. 183. Academic Press, Inc., San Diego, CA.

Bosak T., Bush J.W.M., Flynn M.R., Liang B., Ono S., Petroff A.P., *et al.* (2010) Formation and stability of oxygen-rich bubbles that shape photosynthetic mats. *Geobiology*, **8**, 45–55.

Brush M.J. & Nixon S.W. (2002) Direct measurements of light attenuation by epiphytes on eelgrass *Zostera marina*. *Marine Ecology Progress Series*, **238**, 73–79.

Burkholder J.M. & Wetzel R.G. (1990) Epiphytic alkaline phosphatase on natural and artificial plants in an oligotrophic lake: re-evaluation of the role of macrophytes as a phosphorus source for epiphytes. *Limnology and Oceanography*, **35**, 736–747.

Dade W.B. (1993) Near-bed turbulence and hydrodynamic control of diffusional mass transfer at the sea floor. *Limnology and Oceanography*, **38**, 52–69.

Dodds W.K. (1991) Community interactions between the filamentous alga *Cladophora glomerata* (L.) Kuetzing, its epiphytes, and epiphyte grazers. *Oecologia*, **85**, 572–580.

Dodds W.K. & Biggs B.J.F. (2002) Water velocity attenuation by stream periphyton and macrophytes in relation to growth form and architecture. *Journal of the North American Benthological Society*, **21**, 2–15.

Dodds W.K. & Gudder D.A. (1992) The ecology of *Cladophora*. *Journal of Phycology*, **28**, 415–427.

Drake L.A., Dobbs F.C. & Zimmerman R.C. (2003) Effects of epiphyte load on optical properties and photosynthetic potential of the seagrasses *Thalassia testudinum* Banks ex Konig and *Zostera marina* L. *Limnology and Oceanography*, **48**, 456–463.

Dudley T.L. (1992) Beneficial effects of herbivores on stream macroalgae via epiphyte removal. *Oikos*, **65**, 121–127.

Eminson D. & Moss B. (1980) The composition and ecology of periphyton communities in freshwaters. *British Phycological Journal*, **15**, 429–446.

Enriquez S. & Rodriguez-Roman A. (2006) Effect of water flow on the photosynthesis of three marine macrophytes from a fringing-reef lagoon. *Marine Ecology-Progress Series*, **323**, 119–132.

Escartin J. & Aubrey D.G. (1995) Flow structure and dispersion within algal mats. *Estuarine Coastal and Shelf Science*, **40**, 451–472.

Finlay J.C., Hood J.M., Limm M.P., Power M.E., Schade J.D. & Welter J.R. (2011) Light-mediated thresholds in streamwater nutrient composition in a river network. *Ecology*, **92**, 140–150.

Ghisalberti M. & Nepf H. (2006) The structure of the shear layer in flows over rigid and flexible canopies. *Environmental Fluid Mechanics*, **6**, 277–301.

Ghisalberti M. & Nepf H.M. (2002) Mixing layers and coherent structures in vegetated aquatic flows. *Journal of Geophysical Research-Oceans*, **107**, 3011.

Hardwick A.G.G., Blinn D.W., Usher H.D. & Hardwick G.G. (1992) Epiphytic diatoms on *Cladophora glomerata* in the Colorado River, Arizona: longitudinal and vertical distribution in a regulated river. *The Southwestern Naturalist*, **37**, 148–156.

Hart D.D. (1992) Community organization in streams: The importance of species interactions, physical factors, and chance. *Oecologia*, **91**, 220–228.

Harting J., Kunert C. & Hyvaluoma J. (2010) Lattice Boltzmann simulations in microfluidics: probing the no-slip boundary condition in hydrophobic, rough, and surface nanobubble laden microchannels RID B-4884-2008. *Microfluidics and Nanofluidics*, **8**, 1–10.

Harvey J.W., Noe G.B., Larsen L.G., Nowacki D.J. & McPhillips L.E. (2011) Field flume reveals aquatic vegetation's role in sediment and particulate phosphorus transport in a shallow aquatic ecosystem. *Geomorphology*, **126**, 297–313.

Higgins S.N., Hecky R.E. & Guildford S.J. (2006) Environmental controls of Cladophora growth dynamics in eastern Lake Erie: application of the Cladophora Growth Model (CGM). *Journal of Great Lakes Research*, **32**, 629–644.

Higgins S.N., Hecky R.E. & Guildford S.J. (2008) The collapse of benthic macroalgal blooms in response to self-shading. *Freshwater Biology*, **53**, 2557–2572.

Hurd C.L. (2000) Water motion, marine macroalgal physiology, and production. *Journal of Phycology*, **36**, 453–472.

Hurd C.L., Harrison P.J. & Druehl L.D. (1996) Effect of seawater velocity on inorganic nitrogen uptake by morphologically distinct forms of *Macrocystis integrifolia* from wave-sheltered and exposed sites. *Marine Biology*, **126**, 205–214.

Ikeda S. & Kanazawa M. (1996) Three-dimensional organized vortices above flexible water plants. *Journal of Hydraulic Engineering-ASCE*, **122**, 634–640.

Kays W., Crawford M. & Weigand B. (2005) *Convective Heat and Mass Transfer*. 4th edn. McGraw Hill, Boston, MA, U.S.A.

Koch E.W. (1994) Hydrodynamics, diffusion-boundary layers and photosynthesis of the seagrasses *Thalassia testudinum* and *Cymodocea nodosa*. *Marine Biology*, **118**, 767–776.

Koehler J., Hachol J. & Hilt S. (2010) Regulation of submersed macrophyte biomass in a temperate lowland river: interactions between shading by bank vegetation, epiphyton and water turbidity. *Aquatic Botany*, **92**, 129–136.

Larned S.T., Nikora V.I. & Biggs B.J.F. (2004) Mass-transfer-limited nitrogen and phosphorus uptake by stream periphyton: a conceptual model and experimental evidence. *Limnology and Oceanography*, **49**, 1992–2000.

Leopold L.B. & Maddock T. (1953) The hydraulic geometry of stream channels and some physiographic implications. U.S. *Geological Survey Professional Paper*, **252**, 1–57.

Levich V.G. (1962) *Physiochemical Hydrodynamics*. Prentice-Hall, Englewood Cliffs, NJ.

Losic D., Mitchell J.G. & Voelcker N.H. (2009) Diatomaceous lessons in nanotechnology and advanced materials. *Advanced Materials*, **21**, 2947–2958.

Lowe R.L., Rosen B.H. & Kingston J.C. (1982) A comparison of epiphytes on *Bangia atropurpurea* (Rhodophyta) and *Cladophora glomerata* (Chlorophyta) from northern Lake Michigan. *Ecology of Filamentous Algae*, **8**, 164–168.

Marks J.C. & Power M.E. (2001) Nutrient induced changes in the species composition of epiphytes on *Cladophora glomerata* Kutz. (Chlorophyta). *Hydrobiologia*, **450**, 187–196.

Moeller R.E., Burkholder J.M. & Wetzel R.G. (1988) Significance of sedimentary phosphorus to a rooted submersed macrophyte (*Najas Flexilis* (Willd.) Rostk. and Schmidt) and its algal epiphytes. *Aquatic Botany*, **32**, 261–281.

Moody L.F. (1944) Friction factors for pipe flow. *Transactions of the ASME*, **66**, 671–684.

Nepf H.M. (2012) Flow and transport in regions with aquatic vegetation. *Annual Review of Fluid Mechanics*, **44**, 123–142.

Neto C., Evans D.R., Bonaccurso E., Butt H.J. & Craig V.S.J. (2005) Boundary slip in Newtonian liquids: A review of experimental studies. *Reports on Progress in Physics*, **68**, 2859–2897.

Pal R. (2007) Steady laminar flow of non-Newtonian bubbly suspensions in pipes. *Journal of Non-Newtonian Fluid Mechanics*, **147**, 129–137.

Plew D.R., Cooper G.G. & Callaghan F.M. (2008) Turbulence-induced forces in a freshwater macrophyte canopy. *Water Resources Research*, **44**, W02414.

Power M., Lowe R., Furey P., Welter J., Limm M., Finlay J., et al. (2009) Algal mats and insect emergence in rivers under Mediterranean climates: towards photogrammetric surveillance. *Freshwater Biology*, **54**, 2101–2115.

Power M.E. (1992) Hydrologic and trophic controls of seasonal algal blooms in northern California rivers. *Archivs fur Hydrobiologie*, **125**, 385–410.

Raupach M.R., Finnigan J.J. & Brunet Y. (1996) Coherent eddies and turbulence in vegetation canopies: the mixing-layer analogy. *Boundary-Layer Meteorology*, **78**, 351–382.

Roberts E., Kroker J., Korner S. & Nicklisch A. (2003) The role of periphyton during the re-colonization of a shallow lake with submerged macrophytes. *Hydrobiologia*, **506**, 525–530.

Sand-Jensen K. (1977) Effect of epiphytes on eelgrass photosynthesis. *Aquatic Botany*, **3**, 55–63.

Sand-Jensen K., Binzer T. & Middelboe A.L. (2007) Scaling of photosynthetic production of aquatic macrophytes - a review. *Oikos*, **116**, 280–294.

Sand-Jensen K. & Pedersen O. (1999) Velocity gradients and turbulence around macrophyte stands in streams. *Freshwater Biology*, **42**, 315–328.

Sand-Jensen K., Revsbech N.P. & Jorgensen B.B. (1985) Microprofiles of oxygen in epiphyte communities on submerged macrophytes. *Marine Biology*, **89**, 55–62.

Schanz A., Polte P. & Asmus H. (2002) Cascading effects of hydrodynamics on an epiphyte-grazer system in intertidal seagrass beds of the Wadden Sea. *Marine Biology*, **141**, 287–297.

Shaughnessy E.J., Katz I.M. & Schaffer J.P. (2005) *Introduction to Fluid Mechanics*. Oxford University Press, New York, NY.

Sheng J., Malkiel E. & Katz J. (2006) Digital holographic microscope for measuring three-dimensional particle distributions and motions. *Applied Optics*, **45**, 3893–3901.

Spencer D.F. & Lembi C.A. (1981) Factors regulation the spatial distribution of the filamentous alga Pithophora oedogonia (Chlorophyceae) in an Indiana lake. *Journal of Phycology*, **17**, 168–173.

Steinberger N. & Hondzo M. (1999) Diffusional mass transfer at sediment-water interface. *Journal of Environmental Engineering-ASCE*, **125**, 192–200.

Stevenson J.R. & Peterson C.G. (1991) Emigration and immigration can be important determinants of benthic diatom assemblages in streams. *Freshwater Biology*, **26**, 279–294.

Stewart H.L. & Carpenter R.C. (2003) The effects of morphology and water flow on photosynthesis of marine macroalgae. *Ecology*, **84**, 2999–3012.

Suren A.M. (1991) Bryophytes as invertebrate habitat in two New Zealand alpine streams. *Freshwater Biology*, **26**, 399–418.

Valukina N.V. & Kashinskii O.N. (1979) Investigation of the friction stress on a wall in a monodispensed gas-liquid flow. *Journal of Applied Mechanics and Technical Physics*, **20**, 69–73.

Wheeler W.N. (1980) Effect of boundary-layer transport on the fixation of carbon by the giant kelp *Macrocystis pyrifera*. *Marine Biology*, **56**, 103–110.

Zulkifly S.B., Graham J.M., Young E.B., Mayer R.J., Piotrowski M.J., Smith I., *et al.* (2013) The genus *Cladophora Kützing* (Ulvophyceae) as a globally distributed ecological engineer. *Journal of Phycology*, **49**, 1–17.